ELSEVIER

International Journal of Solids and Structures 41 (2004) 3849–3864

INTERNATIONAL JOURNAL OF SOLIDS and STRUCTURES

www.elsevier.com/locate/ijsolstr

Explicit transient solutions for a mode III crack subjected to dynamic concentrated loading in a piezoelectric material

Yi-Shyong Ing *, Mau-Jung Wang

Department of Aerospace Engineering, Tamkang University, 151, Ying-chuan Road, Tamsui, Taipei, Taiwan 251, ROC

Received 25 September 2003; received in revised form 12 February 2004
Available online 20 March 2004

Abstract

In this study, the transient response of a semi-infinite crack subjected to dynamic anti-plane concentrated loading in a hexagonal piezoelectric medium (6 mm) is investigated. The crack surfaces are assumed to behave as though covered with a conducting electrode. In order to give an insight into the effect of the electrode boundary condition, a simple half-plane problem is also discussed in the paper. A new fundamental solution for piezoelectric materials is proposed and the transient solution for the cracked body is determined by superposition of the fundamental solution in the Laplace transform domain. The fundamental solution to be used is the problem of applying exponentially distributed traction on the crack faces in the Laplace transform domain. Exact analytical transient solutions for the dynamic stress intensity factor, the dynamic electric displacement intensity factor, and the dynamic energy release rate are obtained by using the Cagniard method of Laplace inversion and are expressed in explicit forms. Finally, numerical results for the transient solutions are evaluated and discussed in detail.

Keywords: Crack; Piezoelectric material; Dynamic fracture; Wave propagation

1. Introduction

Recently, due to the intrinsic electro-mechanical coupling behaviors, piezoelectric materials have been widely used as actuating and sensing devices in smart structures. Because of the brittle properties of most piezoelectric materials, the failure analysis of piezoelectric structures has attracted more attention from many researchers. Most of studies, however, are related to static or quasi-static conditions, e.g. Pak (1990), Sosa (1992), Suo et al. (1992), Park and Sun (1995a,b), Zhang and Tong (1996), Narita and Shindo (1998a), Qin and Mai (1998), Gao and Fan (1999a,b), Shen et al. (1999), Yang and Kao (1999), Kwon and Lee (2000), Ru (2000), Gao and Wang (2001), Yang (2001) and Li (2003).

* Corresponding author. Tel.: +886-226-215-656; fax: +886-226-209-746.
E-mail address: ysing@mail.tku.edu.tw (Y.-S. Ing).

0020-7683/$ - see front matter © 2004 Elsevier Ltd. All rights reserved.
doi:10.1016/j.ijsolstr.2004.02.038

Because of the mathematical complications, less attention has been paid to the study of dynamic fracture mechanics of piezoelectric materials. Shindo and Ozawa (1990) first investigated the steady response of a cracked piezoelectric material subjected to plane harmonic waves. Afterward the dynamic fracture analysis of piezoelectric materials is developed rapidly. For example, the single crack problem had been investigated by Chen et al. (1998), Chen (1998), Narita and Shindo (1998b, 1999), Kwon and Lee (2001), Shin et al. (2001), Meguid and Zhao (2002), and Ueda (2003), while the multiple cracks problem had been studied by Wang and Meguid (2000), Wang et al. (2000), Meguid and Chen (2001), Wang (2001), Zhao and Meguid (2002) and Zhou et al. (2003). However, due to the mathematical difficulties, all of the above researchers obtained their solutions by means of some numerical methods. The exactly analytical solution for cracked piezoelectric materials is hard to be derived. Li and Mataga (1996a,b) first obtained transient closed-form solutions for dynamic stress and electric displacement intensities and dynamic energy release rate of a propagating crack in hexagonal piezoelectric materials. They assumed that the crack surfaces are electrode- or vacuum-type boundary conditions and the dynamic anti-plane point loading is initially applied at the stationary crack tip. Hence there is no characteristic length presented in their problems. In this study, the transient response of a semi-infinite crack subjected to dynamic anti-plane concentrated loading on the crack faces in a hexagonal piezoelectric medium is investigated. The inherent characteristic length makes the problem more difficult. A new fundamental solution is derived and the transient solution is determined by superposition of the fundamental solution in the Laplace transform domain. Similar superposition techniques had been successfully used to solve many transient problems of purely elastic solids (Ma and Ing, 1995, 1997a,b; Ing and Ma, 1996, 1997a,b, 1999, 2001, 2003a,b; Ing and Lin, 2002). It demonstrates a powerful method to deal with cracked problems with characteristic lengths.

The choice of conducting or non-conducting boundary conditions of cracked piezoelectric solids is a controversial issue. The types of electric boundary conditions along the crack surfaces have received many discussions in the past researches. How to give suitable consideration to both physical reality and mathematical complications is difficult. In this study, the crack surfaces are assumed to be the electrode-type boundary condition, which shorts out the horizontal component of the electric field at the crack faces but does not affect the mechanical boundary conditions. The same assumption had been proposed by Bleustein (1968) and Li and Mataga (1996a). Although this metallic coating condition is chiefly a mathematically convenient proposition, this boundary condition is also appropriate if the crack surfaces are in a state of electric contact, or if the crack is filled with conducting gas or liquid (Li and Mataga, 1996a). Under this assumption, exact analytical transient solutions for the dynamic stress intensity factor, the dynamic electric displacement intensity factor, and the dynamic energy release rate are obtained in this study. Finally, numerical calculations have been carried out to show the influence of the pertinent parameters.

2. Transient solutions for a piezoelectric half-plane with electrode boundary

Before we deal with the complicated problem of a cracked piezoelectric medium, a simple half-plane problem is studied in order to understand the phenomenon of wave propagation under the electrode boundary condition. If we consider only the out-of-plane displacement and the in-plane electric fields, the dynamic anti-plane governing equations for a hexagonal piezoelectric material (6 mm) can be described by

$$c_{44}\nabla^2 w + e_{15}\nabla^2\phi = \rho\ddot{w}, \tag{1}$$

$$e_{15}\nabla^2 w - \varepsilon_{11}\nabla^2\phi = 0, \tag{2}$$

where $w = w(x, y)$ is the anti-plane displacement in the z-direction (which is assumed to aligned with the hexagonal symmetry axis), $\phi = \phi(x, y)$ is the electric potential, c_{44} is the elastic modulus measured in a constant electric field, ε_{11} is the dielectric permittivity measured at a constant strain, e_{15} is the piezoelectric

constant, and ρ is the material density. $\nabla^2 = \partial^2/\partial x^2 + \partial^2/\partial y^2$ is the in-plane Laplacian and a dot denotes material time derivative.

The constitutive equations for the piezoelectric material can be expressed as (Chen and Karihaloo, 1999)

$$\tau_{kz} = c_{44} w_{,k} + e_{15} \phi_{,k}, \tag{3}$$

$$D_k = e_{15} w_{,k} - \varepsilon_{11} \phi_{,k}, \tag{4}$$

where τ_{kz} and D_k ($k = x, y$) are the anti-plane shear stress and in-plane electric displacements, respectively.

Introduce a transformation proposed by Bleustein (1968)

$$\psi = \phi - \frac{e_{15}}{\varepsilon_{11}} w, \tag{5}$$

the governing equations expressed in Eqs. (1) and (2) can be decoupled as

$$\nabla^2 w = \frac{\rho}{\bar{c}_{44}} \ddot{w}, \tag{6}$$

$$\nabla^2 \psi = 0, \tag{7}$$

where

$$\bar{c}_{44} = c_{44} + \frac{e_{15}^2}{\varepsilon_{11}} \tag{8}$$

is the piezoelectrically stiffened elastic constant. The constitutive equations can then be rewritten as follows:

$$\tau_{kz} = \bar{c}_{44} w_{,k} + e_{15} \psi_{,k}, \tag{9}$$

$$D_k = -\varepsilon_{11} \psi_{,k}. \tag{10}$$

Consider a piezoelectric half-plane occupying the region of $y \leqslant 0$. The free surface $y = 0$ is coated with an infinitesimally thin conducting electrode that is grounded. The piezoelectric half-plane is initially stress-free and at rest. At time $t = 0$, an anti-plane dynamic point loading with magnitude p is applied at the origin $(x, y) = (0, 0)$ on the surface. The boundary conditions of the half-plane problem can be described as follows:

$$\tau_{yz}(x, 0, t) = p\delta(x)H(t), \tag{11}$$

$$\phi(x, 0, t) = 0, \tag{12}$$

where $\delta(\,)$ is the Dirac delta function and $H(\,)$ is the Heaviside function.

This transient problem can be solved by using the integral transform method. The one-sided Laplace transform with respect to time and the two-sided Laplace transform with respect to x are defined by (Achenbach, 1973)

$$\bar{f}(x, y, s) = \int_0^\infty f(x, y, t) \mathrm{e}^{-st} \, \mathrm{d}t, \tag{13}$$

$$\bar{f}^*(\lambda, y, s) = \int_{-\infty}^\infty \bar{f}(x, y, s) \mathrm{e}^{-s\lambda x} \, \mathrm{d}x. \tag{14}$$

Applying the one-sided Laplace transform over time and the two-sided Laplace transform over x in Eqs. (6) and (7), the general solutions for $\bar{w}^*$ and $\bar{\psi}^*$ (in the region of $y \leqslant 0$) in the double transformed domain are

$$\bar{w}^*(\lambda, y, s) = A_1(s, \lambda) \mathrm{e}^{s\alpha(\lambda)y}, \tag{15}$$

$$\bar{\psi}^*(\lambda, y, s) = B_1(s, \lambda)\mathrm{e}^{s\beta(\lambda)y}, \tag{16}$$

where

$$\alpha(\lambda) = (b^2 - \lambda^2)^{1/2}, \tag{17}$$

$$\beta(\lambda) = (\varepsilon^2 - \lambda^2)^{1/2} \tag{18}$$

and

$$b = \sqrt{\frac{\rho}{\bar{c}_{44}}} \tag{19}$$

is the slowness of the bulk shear wave in the piezoelectric material. $\varepsilon \to 0^+$ is an auxiliary positive real perturbation parameter (Li and Mataga, 1996a,b).

From the boundary conditions in Eqs. (11) and (12), we can solved the unknown functions A_1 and B_1. Then the Cagniard method of Laplace inversion (Cagniard, 1939) is employed, the transient full-field solutions for shear stresses and electric displacements can be obtained and expressed in time domain as follows:

$$\tau_{xz}(x, y, t) = \frac{p}{\pi}\left\{\mathrm{Im}\left[\frac{\lambda_1^+}{\alpha(\lambda_1^+) - k_\mathrm{e}^2\beta(\lambda_1^+)}\frac{\partial\lambda_1^+}{\partial t}\right]H(t - br) - k_\mathrm{e}^2\,\mathrm{Im}\left[\frac{\lambda_2^+}{\alpha(\lambda_2^+) - k_\mathrm{e}^2\beta(\lambda_2^+)}\frac{\partial\lambda_2^+}{\partial t}\right]H(t - \varepsilon r)\right\}, \tag{20}$$

$$\tau_{yz}(x, y, t) = \frac{p}{\pi}\left\{\mathrm{Im}\left[\frac{\alpha(\lambda_1^+)}{\alpha(\lambda_1^+) - k_\mathrm{e}^2\beta(\lambda_1^+)}\frac{\partial\lambda_1^+}{\partial t}\right]H(t - br) - k_\mathrm{e}^2\,\mathrm{Im}\left[\frac{\beta(\lambda_2^+)}{\alpha(\lambda_2^+) - k_\mathrm{e}^2\beta(\lambda_2^+)}\frac{\partial\lambda_2^+}{\partial t}\right]H(t - \varepsilon r)\right\}, \tag{21}$$

$$D_x(x, y, t) = \frac{\varepsilon_{11}k_\mathrm{e}^2 p}{e_{15}\pi}\left\{\mathrm{Im}\left[\frac{\lambda_2^+}{\alpha(\lambda_2^+) - k_\mathrm{e}^2\beta(\lambda_2^+)}\frac{\partial\lambda_2^+}{\partial t}\right]H(t - \varepsilon r)\right\}, \tag{22}$$

$$D_x(x, y, t) = \frac{\varepsilon_{11}k_\mathrm{e}^2 p}{e_{15}\pi}\left\{\mathrm{Im}\left[\frac{\beta(\lambda_2^+)}{\alpha(\lambda_2^+) - k_\mathrm{e}^2\beta(\lambda_2^+)}\frac{\partial\lambda_2^+}{\partial t}\right]H(t - \varepsilon r)\right\}, \tag{23}$$

where

$$\lambda_1^+ = -\frac{t}{r}\cos\theta + \mathrm{i}\frac{|\sin\theta|}{r}\sqrt{t^2 - b^2r^2}, \quad \lambda_1^+ = -\frac{t}{r}\cos\theta + \mathrm{i}\frac{|\sin\theta|}{r}\sqrt{t^2 - \varepsilon^2r^2},$$

$$r^2 = x^2 + y^2, \quad \theta = \cos^{-1}\left(\frac{x}{r}\right)$$

and

$$k_\mathrm{e} = \sqrt{\frac{e_{15}^2}{\bar{c}_{44}\varepsilon_{11}}} \tag{24}$$

is the electromechanical coupling coefficient for the electrode boundary condition. It is noted that the function $\alpha - k_\mathrm{e}^2\beta$ in the denominators of Eqs. (20)–(23) corresponds to the Bleustein–Gulyaev piezoelectric surface wave for the electrode-boundary case (Bleustein, 1968; Li and Mataga, 1996a). This surface wave propagates at speed c_{bg} defined by

$$c_{\mathrm{bg}} = \sqrt{\frac{\bar{c}_{44}(1-k_{\mathrm{e}}^4)}{\rho}}. \tag{25}$$

In addition, the appropriate static solutions can be derived by the limiting case $t \to \infty$, and the final results are

$$\tau_{yz}^{\mathrm{s}}(x,y) = \frac{p|\sin\theta|}{\pi r}, \tag{26}$$

$$\tau_{xz}^{\mathrm{s}}(x,y) = \frac{-p\cos\theta}{\pi r}, \tag{27}$$

$$D_x^{\mathrm{s}}(x,y) = \frac{-\varepsilon_{11}k_{\mathrm{e}}^2 p\cos\theta}{e_{15}\pi r(1-k_{\mathrm{e}}^2)}, \tag{28}$$

$$D_y^{\mathrm{s}}(x,y) = \frac{\varepsilon_{11}k_{\mathrm{e}}^2 p|\sin\theta|}{e_{15}\pi r(1-k_{\mathrm{e}}^2)}. \tag{29}$$

The numerical example to be considered here is a PZT-4 half-plane. Fig. 1 shows the non-dimensional transient stresses $\tau_{yz}/\tau_{yz}^{\mathrm{s}}$ for different values of θ. It can be seen that the transient response is non-zero for time $t < br$ (due to the piezoelectric effect) and reveals a square root singularity as the shear wave arrives at the field point, and then approaches to the corresponding static value rapidly. It is noted that, in the case of $\theta = -30°$, there is an obvious variation at the instance $t = 1.15br$ that is the arrival time of the Bleustein–Gulyaev piezoelectric surface wave. In order to observe the characteristic of the surface wave, a field line $\theta = -0.1°$ near the surface is examined and the result is shown in Fig. 2. It is clearly seen that the magnitude of the transient stress tends towards infinity at the arrival time of the surface wave. Hence, the mode III problem of a piezoelectric solid exhibits a similar surface wave phenomenon as the in-plane problem of a purely elastic solid. Fig. 3 shows the non-dimensional electric displacements D_y/D_y^{s} for different values of θ.

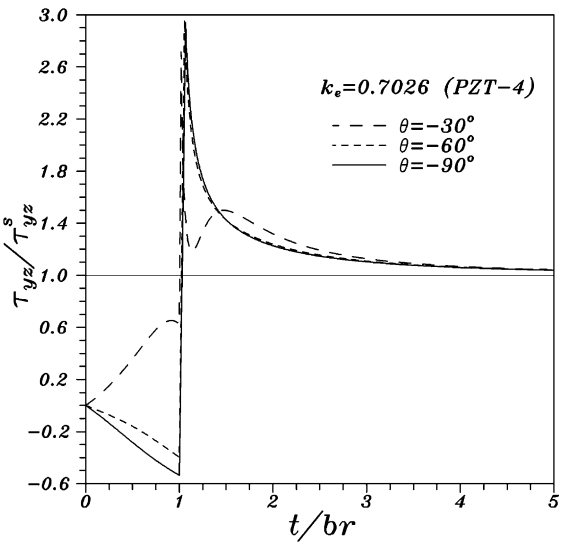

Fig. 1. Transient stresses τ_{yz} of the PZT-4 half-plane for $\theta = -30°$, $-60°$, and $-90°$.

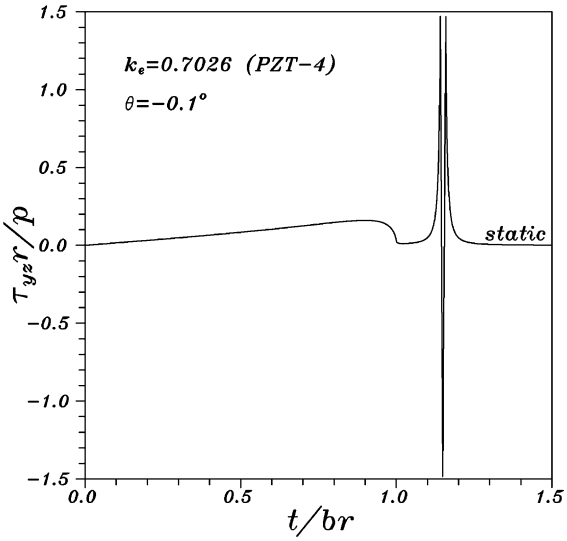

Fig. 2. Transient stresses τ_{yz} of the PZT-4 half-plane for $\theta = -0.1°$.

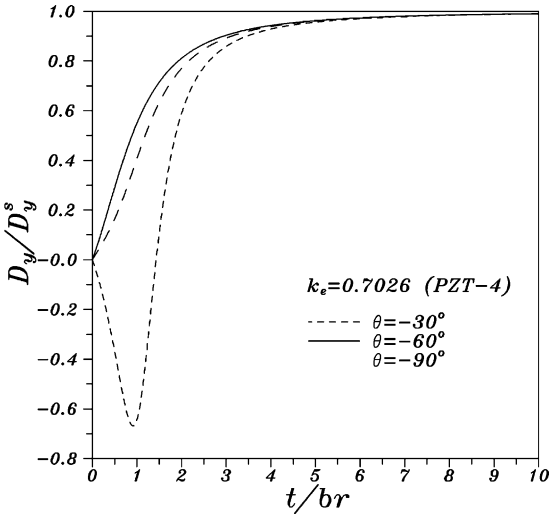

Fig. 3. Transient electric displacements D_y of the PZT-4 half-plane for $\theta = -30°$, $-60°$ and $-90°$.

It can be viewed that there is no singularity at time $t = br$ and the transient response of the electric displacement D_y is always smaller than the corresponding static value.

3. Fundamental solutions for cracked piezoelectric materials

In this section, a fundamental problem is proposed and the associated fundamental solutions will be used to solve the complicatedly cracked problem with a characteristic length in the next section. Consider an unbounded hexagonal piezoelectric medium containing a semi-infinite crack that lies on the negative

x-axis. It is assumed that the crack surfaces are perfectly covered with an infinitesimally thin conducting electrode that is grounded, such that the electrostatic potential vanishes over the crack surfaces. The solutions for an anti-plane exponentially distributed traction applied to the crack faces in the Laplace transform domain will be referred to as the fundamental solutions. Because of the symmetries of the geometry and boundary conditions, this problem can be viewed as a half-plane problem with material occupying the region of $y \geqslant 0$, and subjected to the following mixed boundary conditions in the Laplace transform domain

$$\bar{\tau}_{yz}(x,0,s) = \mathrm{e}^{s\eta x} \quad \text{for } -\infty < x < 0, \tag{30}$$

$$\bar{\phi}(x,0,s) = 0 \quad \text{for } -\infty < x < 0, \tag{31}$$

$$\bar{w}(x,0,s) = 0 \quad \text{for } 0 < x < \infty, \tag{32}$$

where η is a constant.

In order to solve the fundamental problem with the governing equations (6) and (7) and the mixed-type boundary conditions in Eqs. (30)–(32), the integral transform method and the Wiener–Hopf technique will be implemented in the following derivation. From Eqs. (6) and (7), the general solutions for $\bar{w}^*$ and $\bar{\psi}^*$ (in the upper half-plane $y \geqslant 0$) in the double transformed domain can be obtained as follows

$$\bar{w}^*(\lambda,y,s) = A(s,\lambda)\mathrm{e}^{-s\alpha(\lambda)y}, \tag{33}$$

$$\bar{\psi}^*(\lambda,y,s) = B(s,\lambda)\mathrm{e}^{-s\beta(\lambda)y}. \tag{34}$$

Using the relation in Eq. (5) and substituting into the boundary condition in Eq. (31) will have

$$B(s,\lambda) = -\frac{e_{15}}{\varepsilon_{11}}A(s,\lambda). \tag{35}$$

Application of the multiple Laplace transforms to Eqs. (30) and (32) yields

$$\bar{\tau}^*_{yz}(\lambda,0,s) = \frac{1}{s(\eta-\lambda)} + \bar{\tau}^*_+(\lambda,s) \quad \text{for } -\infty < x < \infty, \tag{36}$$

$$\bar{w}^*(\lambda,0,s) = \bar{w}^*_-(\lambda,s) \quad \text{for } -\infty < x < \infty, \tag{37}$$

where $\mathrm{Re}(\eta) > \mathrm{Re}(\lambda)$. The unknown function τ_+ is defined to be the shear stress τ_{yz} on the plane $y = 0$ for $0 < x < \infty$. Likewise, w_- is defined to be the displacement in the z-direction of the crack face $y = 0^+$ for $-\infty < x < 0$. Making use of Eqs. (33) and (37) will lead to $A = \bar{w}^*_-$. From Eqs. (34), (35) and (9), the expression for shear stress $\bar{\tau}^*_{yz}$ is obtained and then substituting it into the transformed stress boundary condition of Eq. (36), we can obtain the following Wiener–Hopf equation:

$$D(\lambda)\bar{w}^*_- = \frac{1}{s^2(\eta-\lambda)} + \frac{\bar{\tau}^*_+}{s}, \tag{38}$$

where

$$D(\lambda) = -\bar{c}_{44}[\alpha(\lambda) - k_e^2\beta(\lambda)]. \tag{39}$$

At this point it is convenient to introduce a new function $S(\lambda)$ by defining

$$S(\lambda) = \frac{1}{1-k_e^2}\frac{\alpha(\lambda) - k_e^2\beta(\lambda)}{\sqrt{b_{bg}+\lambda}\sqrt{b_{bg}-\lambda}}, \tag{40}$$

where $b_{bg} = 1/c_{bg}$ is the slowness of the Bleustein–Gulyaev piezoelectric surface wave for electrode boundary. The function $S(\lambda)$ has the properties that $S(\lambda) \to 1$ as $|\lambda| \to \infty$, and $S(\lambda)$ has neither zeros nor poles in the λ-plane by cuts along $-b_{bg} < \lambda < -\varepsilon$ and $\varepsilon < \lambda < 1/b_{bg}$. From the general product factorization method, $S(\lambda)$ can be written as the product of two regular functions $S_+(\lambda)$ and $S_-(\lambda)$, where

$$S_+(\lambda) = \sqrt{\frac{b_{bg}+\lambda}{b+\lambda}} Q_+(\lambda) \tag{41}$$

and

$$S_-(\lambda) = \sqrt{\frac{b_{bg}-\lambda}{b-\lambda}} Q_-(\lambda), \tag{42}$$

in which

$$Q_+(\lambda) = \exp\left\{ \frac{1}{\pi} \int_\varepsilon^b \tan^{-1}\left[\frac{k_e^2 z}{\alpha(-z)} \right] \frac{dz}{z+\lambda} \right\}. \tag{43}$$

$$Q_-(\lambda) = \exp\left\{ \frac{1}{\pi} \int_\varepsilon^b \tan^{-1}\left[\frac{k_e^2 z}{\alpha(z)} \right] \frac{dz}{z-\lambda} \right\}. \tag{44}$$

In view of the previous discussion, Eq. (38) may be rewritten as

$$-\bar{c}_{44}(1-k_e^2)\frac{(b_{bg}-\lambda)}{\sqrt{(b-\lambda)}} Q_-(\lambda)\bar{w}_-^* = \frac{\sqrt{(b+\lambda)}}{s^2(\eta-\lambda)(b_{bg}+\lambda)Q_+(\lambda)} + \frac{\sqrt{(b+\lambda)}\bar{\tau}_+^*}{s(b_{bg}+\lambda)Q_+(\lambda)}. \tag{45}$$

The first term on the right-hand side is regular for $\mathrm{Re}(\lambda) > -\varepsilon$, except for the pole at $\lambda = \eta$. This pole can, however, be removed by writing

$$\frac{\sqrt{(b+\lambda)}}{s^2(\eta-\lambda)(b_{bg}+\lambda)Q_+(\lambda)} = \frac{\frac{\sqrt{(b+\lambda)}}{(b_{bg}+\lambda)Q_+(\lambda)} - \frac{\sqrt{(b+\eta)}}{(b_{bg}+\eta)Q_+(\eta)}}{s^2(\eta-\lambda)} + \frac{\sqrt{(b+\eta)}}{s^2(\eta-\lambda)(b_{bg}+\eta)Q_+(\eta)}. \tag{46}$$

Eq. (45) can now be rearranged into the desired form

$$\begin{aligned} &-\bar{c}_{44}(1-k_e^2)\frac{(b_{bg}-\lambda)}{\sqrt{(b-\lambda)}} Q_-(\lambda)\bar{w}_-^* - \frac{\sqrt{(b+\eta)}}{s^2(\eta-\lambda)(b_{bg}+\eta)Q_+(\eta)} \\ &\quad = \frac{\sqrt{(b+\lambda)}}{s^2(\eta-\lambda)(b_{bg}+\lambda)Q_+(\lambda)} - \frac{\sqrt{(b+\eta)}}{s^2(\eta-\lambda)(b_{bg}+\eta)Q_+(\eta)} + \frac{\sqrt{(b+\lambda)}\bar{\tau}_+^*}{s(b_{bg}+\lambda)Q_+(\lambda)}. \end{aligned} \tag{47}$$

The left-hand side of this equation is regular for $\mathrm{Re}(\lambda) < 0$, while the right-hand side is regular for $\mathrm{Re}(\lambda) > -\varepsilon$. Applying the analytic continuation argument, therefore, each side of Eq. (47) represents a single entire function, say $E(\lambda)$. By Liouville's theorem, the bounded entire function $E(\lambda)$ is a constant. The magnitude of the constant can be obtained from order conditions on $E(\lambda)$ as $|\lambda| \to \infty$, which in turn are obtained from order conditions on the dependent field variables in the vicinity of $x = 0$. Furthermore, $\bar{\tau}_+(x,0,s)$ is expected to be square root singular near $x = 0$, i.e. $\bar{\tau}_+(x,0,s) = O(|x|^{-1/2})$ as $x \to 0^+$. By using of the Abelian theorem, $E(\lambda)$ vanishes identically, and then we can solve for $\bar{w}_-^*$ from the left-hand side of Eq. (47). Since the amplitude of displacement $A(s,\lambda) = \bar{w}_-^*$ in the Laplace transform domain, we find

$$A(s,\lambda) = -\frac{\sqrt{(b+\eta)(b-\lambda)}}{\bar{c}_{44}(1-k_e^2)s^2(b_{bg}+\eta)Q_+(\eta)(\eta-\lambda)(b_{bg}-\lambda)Q_-(\lambda)}. \tag{48}$$

Substituting Eq. (48) into Eqs. (33)–(35) and making use of Eqs. (9) and (10), and then inverting the two-sided Laplace transform, we can obtain solutions for the fundamental problem in the Laplace transform domain as follows

$$\bar{w}(x,y,s)=\frac{-1}{2\pi \mathrm{i}}\int_{\Gamma_\lambda}\frac{\sqrt{(b+\eta)(b-\lambda)}\mathrm{e}^{-s\alpha(\lambda)y+s\lambda x}}{\bar{c}_{44}(1-k_{\mathrm{e}}^2)s(b_{\mathrm{bg}}+\eta)Q_+(\eta)(\eta-\lambda)(b_{\mathrm{bg}}-\lambda)Q_-(\lambda)}\,\mathrm{d}\lambda, \tag{49}$$

$$\begin{aligned}\bar{\phi}(x,y,s)=&\frac{-1}{2\pi \mathrm{i}}\int_{\Gamma_\lambda}\frac{k_{\mathrm{e}}^2\sqrt{(b+\eta)(b-\lambda)}\mathrm{e}^{-s\alpha(\lambda)y+s\lambda x}}{e_{15}(1-k_{\mathrm{e}}^2)s(b_{\mathrm{bg}}+\eta)Q_+(\eta)(\eta-\lambda)(b_{\mathrm{bg}}-\lambda)Q_-(\lambda)}\,\mathrm{d}\lambda\\&+\frac{1}{2\pi \mathrm{i}}\int_{\Gamma_\lambda}\frac{k_{\mathrm{e}}^2\sqrt{(b+\eta)(b-\lambda)}\mathrm{e}^{-s\beta(\lambda)y+s\lambda x}}{e_{15}(1-k_{\mathrm{e}}^2)s(b_{\mathrm{bg}}+\eta)Q_+(\eta)(\eta-\lambda)(b_{\mathrm{bg}}-\lambda)Q_-(\lambda)}\,\mathrm{d}\lambda,\end{aligned} \tag{50}$$

$$\begin{aligned}\bar{\tau}_{xz}(x,y,s)=&\frac{-1}{2\pi \mathrm{i}}\int_{\Gamma_\lambda}\frac{\sqrt{(b+\eta)(b-\lambda)}\lambda\mathrm{e}^{-s\alpha(\lambda)y+s\lambda x}}{(1-k_{\mathrm{e}}^2)(b_{\mathrm{bg}}+\eta)Q_+(\eta)(\eta-\lambda)(b_{\mathrm{bg}}-\lambda)Q_-(\lambda)}\,\mathrm{d}\lambda\\&+\frac{1}{2\pi \mathrm{i}}\int_{\Gamma_\lambda}\frac{k_{\mathrm{e}}^2\sqrt{(b+\eta)(b-\lambda)}\lambda\mathrm{e}^{-s\beta(\lambda)y+s\lambda x}}{(1-k_{\mathrm{e}}^2)(b_{\mathrm{bg}}+\eta)Q_+(\eta)(\eta-\lambda)(b_{\mathrm{bg}}-\lambda)Q_-(\lambda)}\,\mathrm{d}\lambda,\end{aligned} \tag{51}$$

$$\begin{aligned}\bar{\tau}_{yz}(x,y,s)=&\frac{1}{2\pi \mathrm{i}}\int_{\Gamma_\lambda}\frac{\sqrt{(b+\eta)(b-\lambda)}\alpha(\lambda)\mathrm{e}^{-s\alpha(\lambda)y+s\lambda x}}{(1-k_{\mathrm{e}}^2)(b_{\mathrm{bg}}+\eta)Q_+(\eta)(\eta-\lambda)(b_{\mathrm{bg}}-\lambda)Q_-(\lambda)}\,\mathrm{d}\lambda\\&-\frac{1}{2\pi \mathrm{i}}\int_{\Gamma_\lambda}\frac{k_{\mathrm{e}}^2\sqrt{(b+\eta)(b-\lambda)}\beta(\lambda)\mathrm{e}^{-s\beta(\lambda)y+s\lambda x}}{(1-k_{\mathrm{e}}^2)(b_{\mathrm{bg}}+\eta)Q_+(\eta)(\eta-\lambda)(b_{\mathrm{bg}}-\lambda)Q_-(\lambda)}\,\mathrm{d}\lambda,\end{aligned} \tag{52}$$

$$\overline{D}_x(x,y,s)=-\frac{1}{2\pi \mathrm{i}}\int_{\Gamma_\lambda}\frac{\varepsilon_{11}k_{\mathrm{e}}^2\sqrt{(b+\eta)(b-\lambda)}\lambda\mathrm{e}^{-s\beta(\lambda)y+s\lambda x}}{e_{15}(1-k_{\mathrm{e}}^2)(b_{\mathrm{bg}}+\eta)Q_+(\eta)(\eta-\lambda)(b_{\mathrm{bg}}-\lambda)Q_-(\lambda)}\,\mathrm{d}\lambda, \tag{53}$$

$$\overline{D}_y(x,y,s)=\frac{1}{2\pi \mathrm{i}}\int_{\Gamma_\lambda}\frac{\varepsilon_{11}k_{\mathrm{e}}^2\sqrt{(b+\eta)(b-\lambda)}\beta(\lambda)\mathrm{e}^{-s\beta(\lambda)y+s\lambda x}}{e_{15}(1-k_{\mathrm{e}}^2)(b_{\mathrm{bg}}+\eta)Q_+(\eta)(\eta-\lambda)(b_{\mathrm{bg}}-\lambda)Q_-(\lambda)}\,\mathrm{d}\lambda. \tag{54}$$

The corresponding results of the dynamic stress intensity factor and the electric displacement intensity factor in the Laplace transform domain are

$$\overline{K}_{\mathrm{III}}^{(\tau)}(s)=\lim_{x\to 0}\sqrt{2\pi x}\bar{\tau}_{yz}(x,0,s)=-\frac{\sqrt{2(b+\eta)}}{\sqrt{s}(b_{\mathrm{bg}}+\eta)Q_+(\eta)} \tag{55}$$

and

$$\overline{K}_{\mathrm{III}}^{(D)}(s)=\lim_{x\to 0}\sqrt{2\pi x}\overline{D}_y(x,0,s)=-\frac{\varepsilon_{11}k_{\mathrm{e}}^2\sqrt{2(b+\eta)}}{e_{15}(1-k_{\mathrm{e}}^2)\sqrt{s}(b_{\mathrm{bg}}+\eta)Q_+(\eta)}, \tag{56}$$

respectively.

4. Transient analysis of a piezoelectric crack subjected to dynamic concentrated loading

Consider a semi-infinite crack located at $y=0, x<0$ in an unbounded hexagonal piezoelectric medium as shown in Fig. 4. It is assumed that the crack surfaces are completely coated with an infinitesimally thin perfectly conducting electrode that is grounded, such that the electrostatic potential vanishes over the crack

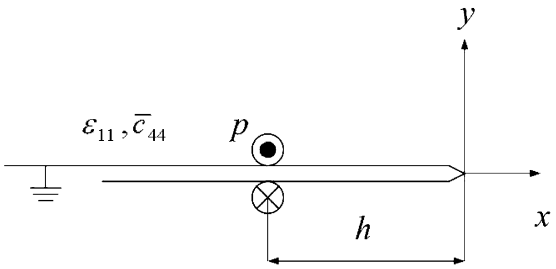

Fig. 4. Configuration and coordinate system of a piezoelectric crack subjected to anti-plane shear forces.

surfaces. At time $t = 0$, a pair of equal and opposite dynamic anti-plane concentrated loadings with magnitude p are applied at the crack faces with a distance h from the crack tip. The time dependence of the concentrated loading is represented by the Heaviside function $H(t)$. The boundary condition for the applied loading can be represented by

$$\tau_{yz}(x, 0, t) = -p\delta(x + h)H(t). \tag{57}$$

The incident field generated by the concentrated loading can be expressed in the Laplace transform domain as follows:

$$\bar{\tau}_{yz}(x, 0, s) = \frac{1}{2\pi \mathrm{i}} \int_{\Gamma_\lambda} -p\mathrm{e}^{s\lambda(h+x)}\,\mathrm{d}\lambda. \tag{58}$$

The applied traction on the crack faces as indicated in Eq. (58), has the functional form $\mathrm{e}^{s\lambda x}$. Since the solutions of applying traction $\mathrm{e}^{s\eta x}$ on crack faces have been solved in the previous section, the diffracted field generated from the crack tip can be constructed by superimposing the incident wave traction that is equal to Eq. (58). Since the dynamic stress and electric displacement intensities and the dynamic energy release rate are the key parameters in characterizing dynamic crack growth, we will focus our attention mainly on the determination of these quantities. When we combine Eqs. (55) and (58), the dynamic stress intensity factor expressed in the Laplace transform domain can be obtained as follows:

$$\overline{K}_{\mathrm{III}}^{(\tau)}(s) = \frac{1}{2\pi \mathrm{i}} \int_{\Gamma_\lambda} -p\mathrm{e}^{s\lambda h} \left\{ -\frac{\sqrt{2(b+\lambda)}}{\sqrt{s}(b_{\mathrm{bg}} + \lambda)Q_+(\lambda)} \right\} \mathrm{d}\lambda \tag{59}$$

and from Eqs. (56) and (58), the dynamic electric displacement intensity factor is

$$\overline{K}_{\mathrm{III}}^{(D)}(s) = \frac{1}{2\pi \mathrm{i}} \int_{\Gamma_\lambda} -p\mathrm{e}^{s\lambda h} \left\{ -\frac{\varepsilon_{11} k_{\mathrm{e}}^2 \sqrt{2(b+\lambda)}}{e_{15}(1-k_{\mathrm{e}}^2)\sqrt{s}(b_{\mathrm{bg}} + \lambda)Q_+(\lambda)} \right\} \mathrm{d}\lambda. \tag{60}$$

By using the Cagniard method of Laplace inversion, the relevant dynamic intensity factors in time domain can be obtained as follows

$$K_{\mathrm{III}}^{(\tau)}(t) = \sqrt{\frac{2}{\pi^3 h}} p \int_0^t \mathrm{Re}\left[\frac{\sqrt{\tau - b\bar{h}}}{(\tau - b_{\mathrm{bg}}h)Q_-(\tau/h)\sqrt{t-\tau}} \right] \mathrm{d}\tau\ H(t) \tag{61}$$

and

$$K_{\mathrm{III}}^{(D)}(t) = \frac{\varepsilon_{11} k_{\mathrm{e}}^2}{e_{15}(1-k_{\mathrm{e}}^2)} \sqrt{\frac{2}{\pi^3 h}} p \int_0^t \mathrm{Re}\left[\frac{\sqrt{\tau - b\bar{h}}}{(\tau - b_{\mathrm{bg}}h)Q_-(\tau/h)\sqrt{t-\tau}} \right] \mathrm{d}\tau\ H(t). \tag{62}$$

It is pointed out that the integrands in the brackets of Eqs. (61) and (62) are purely imaginary numbers when $t < bh$, so the dynamic intensity factors equal zero during this stage. The reason is that for the particular case of the electrode boundary condition considered here, the electrostatic potential is zero not only on the crack face but also along the line ahead of the crack. Consequently, there is no effect from electric field to the dynamic intensity factors before the incident shear wave is diffracted by the crack tip. Furthermore, both integrands of Eqs. (61) and (62) have a pole singularity at $\tau = b_{\mathrm{bg}}h$, which corresponds to the instant of arrival of the Bleustein-Gulyaev piezoelectric surface wave traveling along the crack faces from the load points to the crack tip. The direct calculations cannot be applied to these integrals for $t > b_{\mathrm{bg}}h$. By using contour integration, however, the integrals in Eqs. (61) and (62) for time $t > b_{\mathrm{bg}}h$ can be evaluated and yield

$$K_{\mathrm{III}}^{(\tau)}(t) = K_{\mathrm{III}}^{(\tau),s} H(t - b_{\mathrm{bg}}h), \tag{63}$$

$$K_{\mathrm{III}}^{(D)}(t) = K_{\mathrm{III}}^{(D),s} H(t - b_{\mathrm{bg}}h), \tag{64}$$

where

$$K_{\mathrm{III}}^{(\tau),s} = p\sqrt{\frac{2}{\pi h}} \tag{65}$$

and

$$K_{\mathrm{III}}^{(D),s} = \frac{\varepsilon_{11}k_{\mathrm{e}}^2 p}{e_{15}(1-k_{\mathrm{e}}^2)}\sqrt{\frac{2}{\pi h}}. \tag{66}$$

The results expressed in Eqs. (65) and (66) are the corresponding static solutions of the stress intensity factor and the electric displacement intensity factor, respectively. It is interesting to note that the magnitude of both dynamic intensity factors jumps from infinity to the appropriate static value right after the Bleustein–Gulyaev piezoelectric surface wave passes through the crack tip.

The energy release rate is an alternatively important quantity in fracture mechanics. According to the above mention, there is no contribution from electric field to the dynamic energy release rate because of the special electrode boundary condition. The energy release rate can be calculated in a way similar to the purely elastic case. From Freund (1972), the energy release rate can be computed by

$$\begin{aligned} G(t) &\equiv 2\lim_{a\to 0}\int_{-a}^{a}\left[\tau_{yz}(x,0,t)\frac{\partial w}{\partial x}(x,0,t) + D_y(x,0,t)\frac{\partial \phi}{\partial x}(x,0,t)\right]\mathrm{d}x \\ &= 2\lim_{a\to 0}\int_{-a}^{a}\tau_{yz}(x,0,t)\frac{\partial w}{\partial x}(x,0,t)\,\mathrm{d}x. \end{aligned} \tag{67}$$

In order to calculate the dynamic energy release rate, the shear stress τ_{yz} and displacement w along $y = 0$ should be obtained first. Combining Eq. (58) and the fundamental solutions expressed in Eqs. (49) and (52), the anti-plane displacement $\bar{w}$ and shear stress $\bar{\tau}_{yz}$ represented in the Laplace transform domain can be derived as follows:

$$\begin{aligned} \bar{w}(x,y,s) = {} & \frac{1}{2\pi \mathrm{i}}\int_{\Gamma_{\eta_1}} -p\mathrm{e}^{s\eta_1 h}\,\mathrm{d}\eta_1 \\ & \times\left\{\frac{-1}{2\pi \mathrm{i}}\int_{\Gamma_{\eta_2}}\frac{\sqrt{(b+\eta_1)(b-\eta_2)}\mathrm{e}^{-s\alpha(\eta_2)y+s\eta_2 x}}{\bar{c}_{44}(1-k_{\mathrm{e}}^2)s(b_{\mathrm{bg}}+\eta_1)Q_+(\eta_1)(\eta_1-\eta_2)(b_{\mathrm{bg}}-\eta_2)Q_-(\eta_2)}\,\mathrm{d}\eta_2\right\}, \end{aligned} \tag{68}$$

$$\bar{\tau}_{yz}(x,y,s)=\frac{1}{2\pi \mathrm{i}}\int_{\Gamma_{\eta_1}}-p\mathrm{e}^{s\eta_1 h}\,\mathrm{d}\eta_1\times\left\{\frac{1}{2\pi \mathrm{i}}\int_{\Gamma_{\eta_2}}\frac{\sqrt{(b+\eta_1)(b-\eta_2)}\alpha(\eta_2)\mathrm{e}^{-s\alpha(\eta_2)y+s\eta_2 x}}{(1-k_{\mathrm{e}}^2)(b_{\mathrm{bg}}+\eta_1)Q_+(\eta_1)(\eta_1-\eta_2)(b_{\mathrm{bg}}-\eta_2)Q_-(\eta_2)}\,\mathrm{d}\eta_2\right.$$
$$\left.-\frac{1}{2\pi \mathrm{i}}\int_{\Gamma_{\eta_2}}\frac{k_{\mathrm{e}}^2\sqrt{(b+\eta_1)(b-\eta_2)}\beta(\eta_2)\mathrm{e}^{-s\beta(\eta_2)y+s\eta_2 x}}{(1-k_{\mathrm{e}}^2)(b_{\mathrm{bg}}+\eta_1)Q_+(\eta_1)(\eta_1-\eta_2)(b_{\mathrm{bg}}-\eta_2)Q_-(\eta_2)}\,\mathrm{d}\eta_2\right\}. \tag{69}$$

By setting $y=0$, inverting the Laplace transform, and then taking the limit $x\to 0$, we can obtain

$$\lim_{x\to 0}\frac{\partial w}{\partial x}(x,0,t)=\frac{p}{\pi^2\bar{c}_{44}(1-k_{\mathrm{e}}^2)\sqrt{h}}\lim_{x\to 0}\int_0^t \mathrm{Re}\left[\frac{\sqrt{\tau-b\bar{h}}H(-x)}{(\tau-b_{\mathrm{bg}}h)Q_-(\tau/h)\sqrt{t-\tau}\sqrt{-x}}\right]\mathrm{d}\tau, \tag{70}$$

$$\lim_{x\to 0}\tau_{yz}(x,0,t)=\frac{p}{\pi^2\sqrt{h}}\lim_{x\to 0}\int_0^t \mathrm{Re}\left[\frac{\sqrt{\tau-b\bar{h}}H(x)}{(\tau-b_{\mathrm{bg}}h)Q_-(\tau/h)\sqrt{t-\tau}\sqrt{x}}\right]\mathrm{d}\tau. \tag{71}$$

Substituting Eqs. (70) and (71) into Eq. (67), and making use of the identity (Freund, 1972)

$$\lim_{a\to 0}\int_{-a}^{a}\frac{H(x)}{\sqrt{x}}\frac{H(-x)}{\sqrt{-x}}\,\mathrm{d}x=\frac{\pi}{2}, \tag{72}$$

the dynamic energy release rate can be obtained as follows:

$$G(t)=\frac{p^2}{\pi^3 h\bar{c}_{44}(1-k_{\mathrm{e}}^2)}\left\{\int_0^t \mathrm{Re}\left[\frac{\sqrt{\tau-b\bar{h}}}{(\tau-b_{\mathrm{bg}}h)Q_-(\tau/h)\sqrt{t-\tau}}\right]\mathrm{d}\tau\right\}^2=\frac{1}{2\bar{c}_{44}(1-k_{\mathrm{e}}^2)}[K_{\mathrm{III}}^{(\tau)}(t)]^2. \tag{73}$$

This expression is the same as the solution in Eq. (156) of Li and Mataga (1996a) (by setting $v=0$). As $k_{\mathrm{e}}\to 0$, Eq. (73) reduces to the well-known purely elastic results

$$G(t)=\frac{1}{2c_{44}}[K_{\mathrm{III}}^{(\tau)}(t)]^2. \tag{74}$$

Next numerical calculations have been carried out to show the influence of the pertinent parameters. Three piezoelectric materials, PZT-4, $BaTiO_3$, and PZT-5, are chosen for numerical evaluations. The material properties of these three piezoelectric media are given in Table 1. Fig. 5 shows the variation of the dynamic stress intensity factors with the normalized time t/bh. Since the electrostatic potential is zero along the entire line $y=0$, the transient solution keeps zero before the shear wave arrives at the crack tip ($t<bh$). Afterward it decreases violently during the stage $bh<t<b_{\mathrm{bg}}h$, and reveals a singularity as the Bleustein–Gulyaev piezoelectric surface wave arrives at the crack tip ($t=b_{\mathrm{bg}}h$), and then jumps immediately to the static value when the surface wave passes through the tip. As indicated in Eq. (65), the static solution is independent of material properties.

Fig. 6 shows the transient responses of the dynamic electric displacement intensity factors. The transient behavior is similar to that of the dynamic stress intensity factor. However, the jumped values for static solutions are not the same for different piezoelectric materials after the surface wave passes the crack tip.

Table 1
Material properties of PZT-4, $BaTiO_3$, and PZT-5 piezoelectric media (Li and Mataga, 1996a)

Compound	PZT-4	$BaTiO_3$	PZT-5
ρ (kg/m^3)	7500	5700	7750
c_{44} (10^{10} N/m^3)	2.56	4.4	2.11
ε_{11} (10^{-10} C/V m)	64.634	98.722	81.103
e_{15} (C/m^2)	12.7	11.4	12.3

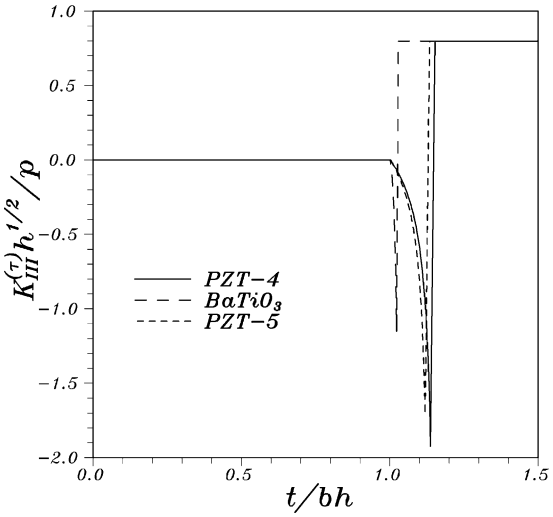

Fig. 5. Normalized dynamic stress intensity factors versus normalized time for various piezoelectric materials.

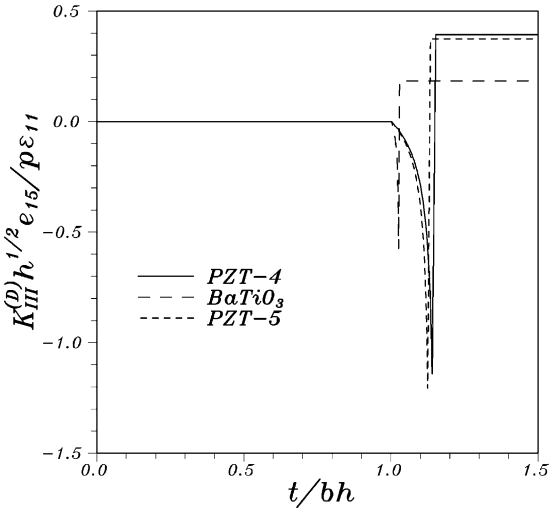

Fig. 6. Normalized dynamic electric displacement intensity factors versus normalized time for various piezoelectric materials.

The transient responses of the dynamic energy release rates are plotted in Fig. 7. It can be seen that the dynamic energy release rate also jumps to a constant value as the surface wave passes the crack tip. Furthermore, in view of Eq. (73), the value of energy release rate increases with k_e while decreases with $\bar{c}_{44}$. However, since $k_e = \sqrt{e_{15}^2/(\bar{c}_{44}\varepsilon_{11})}$, the overall effect is to increase the energy release rate with increasing k_e (or with decreasing $\bar{c}_{44}$) for fixed $e_{15}^2/\varepsilon_{11}$. Reexamining Eq. (8), $\bar{c}_{44} = c_{44} + (e_{15}^2/\varepsilon_{11})$, so the elastic modulus c_{44} dominates dynamic energy release rate over the ratio of $e_{15}^2/\varepsilon_{11}$.

So far, the solutions for dynamic intensities and energy release rate of a piezoelectric crack subjected to a pair of concentrated loadings on crack faces have been derived. It is noted that the solutions for more general crack face loading can be obtained on the basis of the results shown in Eqs. (61), (62) and (73).

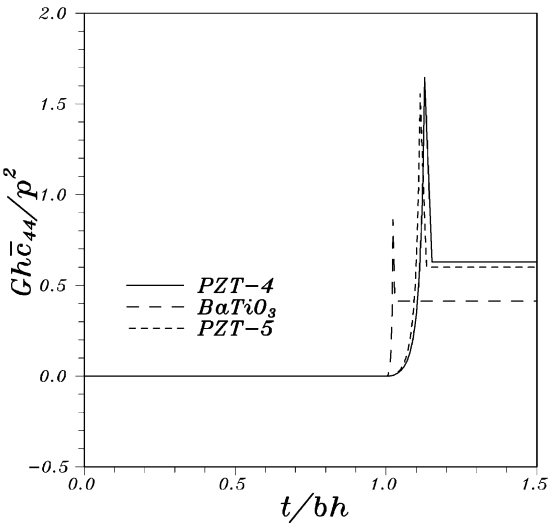

Fig. 7. Normalized dynamic energy release rates normalized time for various piezoelectric materials.

Suppose that the crack faces are loaded by a pair of concentrated dynamic loadings applied at $x = -h$ with time dependent $pg(t)$ and $g(t) = 0$ for $t < 0$. The dynamic stress intensity factor for this modified problem is

$$K_{\mathrm{III}}^{(\tau),g}(t) = \int_0^t K_{\mathrm{III}}^{(\tau)}(t-\xi)\dot{g}(\xi)\,\mathrm{d}\xi. \tag{75}$$

However, if a traction distribution $pf(x)$ is suddenly applied over the interval $x_1 < x < x_2$ on crack faces, then the transient stress intensity factor of the problem is

$$K_{\mathrm{III}}^{(\tau),f}(t) = \int_{x_1}^{x_2} K_{\mathrm{III}}^{(\tau)}(t;x)f(x)\,\mathrm{d}x. \tag{76}$$

Although the general results may directly be evaluated by integration from Eqs. (75) and (76), the superposition method just mentioned can be followed by applying the fundamental solution in Section 3. For instance, for the case when sudden uniform load $\tau_{yz}(x,0,t) = -\tau_0 H(-x)H(t)$ is applied on the entire crack surfaces, the dynamic stress intensity factor can be obtained by using the fundamental solution in Eq. (55). The final result of dynamic stress intensity factor in time domain is

$$K_{\mathrm{III}}^{(\tau),\mathrm{uniform}}(t) = \frac{2\tau_0}{b_{\mathrm{bg}}Q_+(0)}\sqrt{\frac{2bt}{\pi}}. \tag{77}$$

Because the permeable boundary condition on crack surfaces is assumed in this study, the presence of electric loading on crack surfaces is not allowable. Equation (77) indicates that dynamic stress intensity factor is always positive and proportional to $\sqrt{t}$ under uniform shear load. A similar phenomenon can be observed in Fig. 2 ($D_0 = 0, t < 2c_2a$) of Chen and Karihaloo (1999) for the impermeable case.

5. Conclusions

The transient response of a cracked piezoelectric medium subjected to dynamic anti-plane concentrated loading has been investigated. It is assumed that the crack surfaces are coated with an infinitesimally thin

conducting electrode that is grounded. A new fundamental solution for piezoelectric materials is derived and the transient solutions are determined by superposition of the fundamental solution in the Laplace transform domain. Exact analytical transient solutions for the dynamic stress intensity factor, the dynamic electric displacement intensity factor, and the dynamic energy release rate are obtained and expressed in explicit forms. The solution obtained in this paper can be considered to be a Green function for the associated problem. The solutions to problems of any arbitrary spatially distributed loading, or more general time dependence, can be obtained by superposition. Furthermore, this method can be extended to solve more complicatedly piezoelectric problems involving crack propagation or other boundary effects. The results will be shown in a future paper.

Acknowledgements

The authors gratefully acknowledge the financial support of this research by the National Science Council (Republic of China) under Grant NSC 91-2212-E-032-002.

References

Achenbach, J.D., 1973. Wave Propagation in Elastic Solids. Elsevier, New York.

Bleustein, J.L., 1968. A new surface wave in piezoelectric materials. Applied Physics Letters 13, 412–413.

Cagniard, L., 1939. Reflexion et Refraction des Ondes Seismiques Progressives. Cauthiers-Villars, Paris (Translated into English and revised by Flinn, E.A., Dix, C.H., 1962. Reflection and Refraction of Progressive Seismic Waves. McGraw-Hill, New York).

Chen, Z.T., 1998. Crack tip field of an infinite piezoelectric strip under anti-plane impact. Mechanics Research Communications 25, 313–319.

Chen, Z.T., Karihaloo, B.L., 1999. Dynamic response of a cracked piezoelectric ceramic under arbitrary electro-mechanical impact. International Journal of Solids and Structures 36, 5125–5133.

Chen, Z.T., Karihaloo, B.L., Yu, S.W., 1998. A Griffith crack moving along the interface of two dissimilar piezoelectric materials. International Journal of Fracture 91, 197–203.

Freund, L.B., 1972. Energy flux into the tip of an extending crack in an elastic solid. Journal of Elasticity 2, 341–349.

Gao, C.F., Fan, W.X., 1999a. A general solution for the plane problem in piezoelectric media with collinear cracks. International Journal of Engineering Science 37, 347–363.

Gao, C.F., Fan, W.X., 1999b. Exact solutions for the inplane problem in piezoelectric materials with an elliptic or a crack. International Journal of Solids and Structures 36, 2527–2540.

Gao, C.F., Wang, M.Z., 2001. Green's functions of an interfacial crack between two dissimilar piezoelectric media. International Journal of Solids and Structures 38, 5323–5334.

Ing, Y.S., Lin, J.T., 2002. Dynamic full-field analysis of a surface crack subjected to an antiplane moving loading. Journal of the Chinese Institute of Engineers 25, 639–651.

Ing, Y.S., Ma, C.C., 1996. Transient response of a finite crack subjected to dynamic antiplane loading. International Journal of Fracture 82, 345–362.

Ing, Y.S., Ma, C.C., 1997a. Dynamic fracture analysis of a finite crack subjected to an incident horizontally polarized shear wave. International Journal of Solids and Structures 34, 895–910.

Ing, Y.S., Ma, C.C., 1997b. Transient analysis of a subsonic propagating interface crack subjected to anti-plane dynamic loading in dissimilar isotropic materials. Journal of Applied Mechanics 64, 546–556.

Ing, Y.S., Ma, C.C., 1999. Transient analysis of a propagating crack with finite length subjected to a horizontally polarized shear wave. International Journal of Solids and Structures 36, 4609–4627.

Ing, Y.S., Ma, C.C., 2001. Transient response of a surface crack subjected to dynamic anti-plane concentrated loadings. International Journal of Fracture 109, 239–261.

Ing, Y.S., Ma, C.C., 2003a. Dynamic fracture analysis of finite cracks by horizontally polarized shear waves in anisotropic solids. Journal of the Mechanics and Physics of Solids 51, 1987–2021.

Ing, Y.S., Ma, C.C., 2003b. Full-field analysis of an anisotropic finite crack subjected to an anti-plane point impact loading (submitted).

Kwon, S.M., Lee, K.Y., 2000. Analysis of stress and electric field in a rectangular piezoelectric body with a center crack under anti-plane shear loading. International Journal of Solids and Structures 37, 4859–4869.

Kwon, S.M., Lee, K.Y., 2001. Transient response of a rectangular piezoelectric medium with a center crack. European Journal of Mechanics A/Solids 20, 457–468.

Li, S., 2003. On global energy release rate of a permeable crack in a piezoelectric ceramic. Journal of Applied Mechanics 70, 246–252.

Li, S., Mataga, P.A., 1996a. Dynamic crack propagation in piezoelectric materials—Part I. Electrode solution. Journal of the Mechanics and Physics of Solids 44, 1799–1830.

Li, S., Mataga, P.A., 1996b. Dynamic crack propagation in piezoelectric materials—Part II. Vacuum solution. Journal of the Mechanics and Physics of Solids 44, 1831–1866.

Ma, C.C., Ing, Y.S., 1995. Transient analysis of dynamic crack propagation with boundary effect. Journal of Applied Mechanics 62, 1029–1038.

Ma, C.C., Ing, Y.S., 1997a. Dynamic crack propagation in a layered medium under antiplane shear. Journal of Applied Mechanics 64, 66–72.

Ma, C.C., Ing, Y.S., 1997b. Transient analysis of a crack in a composite layered medium subjected to dynamic loadings. AIAA Journal 35, 706–711.

Meguid, S.A., Chen, Z.T., 2001. Transient response of a finite piezoelectric strip containing coplanar insulating cracks under electromechanical impact. Mechanics of Materials 33, 85–96.

Meguid, S.A., Zhao, X., 2002. The interface crack problem of bonded piezoelectric and elastic half-space under transient electromechanical loads. Journal of Applied Mechanics 69, 244–253.

Narita, F., Shindo, Y., 1998a. Layered piezoelectric medium with interface crack under anti-plane shear. Theoretical and Applied Fracture Mechanics 30, 119–126.

Narita, F., Shindo, Y., 1998b. Dynamic anti-plane shear of a cracked piezoelectric ceramic. Theoretical and Applied Fracture Mechanics 29, 169–180.

Narita, F., Shindo, Y., 1999. Scattering of antiplane shear waves by a finite crack in piezoelectric laminates. Acta Mechanica 134, 27–43.

Pak, Y.E., 1990. Crack extension force in a piezoelectric material. Journal of Applied Mechanics 57, 647–653.

Park, S.B., Sun, C.T., 1995a. Effect of electric field on fracture of piezoelectric ceramics. International Journal of Fracture 70, 203–216.

Park, S.B., Sun, C.T., 1995b. Fracture criteria of piezoelectric ceramics. Journal- American Ceramic Society 78, 1475–1480.

Qin, Q.H., Mai, Y.W., 1998. Multiple cracks in thermoelectroelastic bimaterials. Theoretical and Applied Fracture Mechanics 29, 141–150.

Ru, C.Q., 2000. Exact solution for finite electrode layers embedded at the interface of two piezoelectric half-planes. Journal of Mechanics and Physics of Solids 48, 693–708.

Shen, S., Kuang, Z.B., Hu, S., 1999. Interface crack problems of a laminated piezoelectric plate. European Journal of Mechanics A/Solids 18, 219–238.

Shin, J.W., Kwon, S.M., Lee, K.Y., 2001. An eccentric crack in a piezoelectric strip under anti-plane shear impact loading. International Journal of Solids and Structures 38, 1483–1494.

Shindo, Y., Ozawa, E., 1990. Dynamic analysis of a piezoelectric material. In: Hsieh, R.K.T. (Ed.), Mechanical Modeling of New Electromagnetic Materials. Elsevier, Amsterdam, pp. 297–304.

Sosa, H., 1992. On the fracture mechanics of piezoelectric solids. International Journal of Solids and Structures 29, 2613–2622.

Suo, Z., Kuo, C.M., Barnett, D.M., Willis, J.R., 1992. Fracture mechanics of piezoelectric ceramics. Journal of the Mechanics and Physics of Solids 40, 739–765.

Ueda, S., 2003. Diffraction of antiplane shear waves in a piezoelectric laminate with a vertical crack. European Journal of Mechanics A/Solids 22, 413–422.

Wang, B.L., Han, J.C., Du, S.Y., 2000. Electroelastic fracture dynamics for multilayered piezoelectric materials under dynamic anti-plane shearing. International Journal of Solids and Structures 37, 5219–5231.

Wang, X.D., 2001. On the dynamic behaviour of interacting interfacial cracks in piezoelectric media. International Journal of Solids and Structures 38, 815–831.

Wang, X.D., Meguid, S.A., 2000. Modelling and analysis of the dynamic behaviour of piezoelectric materials containing interacting cracks. Mechanics of Materials 32, p. 723, 737.

Yang, F., 2001. Fracture mechanics for a mode I crack in piezoelectric materials. International Journal of Solids and Structures 38, 3813–3830.

Yang, F., Kao, I., 1999. Crack problem in piezoelectric materials: general anti-plane mechanical loading. Mechanics of Materials 31, 395–406.

Zhang, T.Y., Tong, P., 1996. Fracture mechanics for mode III crack in a piezoelectric material. International Journal of Solids and Structures 33, 343–359.

Zhao, X., Meguid, S.A., 2002. On the dynamic behaviour of a piezoelectric laminate with multiple interfacial collinear cracks. International Journal of Solids and Structures 39, 2477–2494.

Zhou, Z.G., Wang, B., Sun, Y.G., 2003. Investigation of the dynamic behavior of two parallel symmetric cracks in piezoelectric materials use of non-local theory. International Journal of Solids and Structures 40, 747–762.